Wavelike Nature of van der Waals Interactions at the Nanoscale

Alberto Ambrosetti[1,2], Nicola Ferri[1], Robert A. DiStasio Jr.[3], and Alexandre Tkatchenko[1,4]
[1] *Fritz-Haber-Institut der Max-Planck-Gesellschaft, Faradayweg 4-6, D-14195, Berlin, Germany*
[2] *Dipartimento di Fisica e Astronomia, Universitá degli Studi di Padova, via Marzolo 8, 35131, Padova, Italy*
[3] *Department of Chemistry and Chemical Biology, Cornell University, Ithaca, NY 14853, USA*
[4] *Physics and Materials Science Research Unit, University of Luxembourg, L-1511 Luxembourg*

The concept of wave-particle duality is one of the cornerstones of quantum mechanics. As such, the most commonly utilized particle- or fragment-based models for describing van der Waals (vdW) dispersion interactions—forces which are ubiquitous in nature and quantum mechanical in origin—are incomplete by construction. This observation is exemplified by recent experimental investigations of non-covalent forces at the nanoscale, which have challenged the basic assumptions of such particle-based models and await an accurate and physically sound theoretical explanation. In this work, we demonstrate that a qualitatively correct description of vdW interactions between polarizable nanostructures over a wide range of *finite distances* can only be attained by accounting for the delocalized wavelike nature of electron density fluctuations. By considering a diverse set of nanoscale and biological systems with markedly different underlying dimensionalities, topologies, and polarizabilities, we find a visible enhancement in the non-locality of the charge density response on the range of 10–20 nm; furthermore, it is these collective wavelike fluctuations that are responsible for the emergence of non-trivial interaction power laws. The wavelike nature of vdW interactions provides a hitherto unexplored avenue towards understanding the structure and assembly of complex polarizable nanostructures.

The assembly of complex nanostructures and biological systems from simpler building blocks is often driven by non-covalent van der Waals (vdW) or dispersion interactions, quantum mechanical phenomena that are ubiquitous in nature and arise from electrodynamic correlations between instantaneous charge fluctuations in matter [1]. In fact, it has become increasingly more apparent that vdW forces have an influence which extends well beyond binding energies, and encompasses the structural [2, 3], mechanical [4, 5], spectroscopic [6], and even electronic [7] signatures of condensed matter. As such, even a slight variation in the power laws that govern the magnitude of these ubiquitous interactions as a function of the separation between two or more objects (*e.g.*, atoms, molecules, nanostructures, surfaces, or solids) can have a profound impact on their observed properties and therefore demands an accurate, physically sound theoretical description.

Thus far, both our conceptual understanding of vdW interactions and the quantitative models widely employed for describing these quantum mechanical phenomena are primarily rooted in low-order intermolecular perturbation theory (IPT), wherein vdW binding originates from the interactions between transient local multipoles [8]. While such theories have had enormous success in describing vdW binding in (small) gas-phase molecular systems, recent advanced experimental techniques have produced several findings that are challenging the basic assumptions of IPT for nanostructured materials and are strongly indicative that even our *qualitative* understanding of vdW interactions is incomplete and needs to be substantially revised [9]. Examples of such experimental observations include: (*i*) ultra long-range vdW interactions extending up to tens of nm into heterogeneous dielectric interfaces [10, 11], (*ii*) complete screening of the vdW interaction between an atomic force microscope (AFM) tip and a SiO_2 surface by the presence of a single (or a few) layer(s) of graphene adsorbed on the surface [12], (*iii*) super-linear sticking power laws for the self-assembly of metallic clusters on carbon nanotubes with increasing surface area [13], and (*iv*) non-linear increases in the vdW attraction between homologous molecules and an Au(111) surface as a function of the molecular size [14]. Satisfactory theoretical explanations for these experimental findings require either *ad hoc* modifications to IPT [(*iii*) and (*iv*)] or are inherently outside the domain of applicability of IPT [(*i*) and (*ii*)].

To address these issues, we first note that the spatial extent of the instantaneous charge density fluctuations responsible for vdW interactions depends rather sensitively on the nature and character of the occupied–to–virtual transitions of the valence electrons in a given molecule or material. In this regard, it is well-known that the inherent delocalization characteristic of low-dimensional metallic systems leads to a remarkably slow decay in the interaction energies between metallic chains and layers as a function of their separation [15], a modification of the "conventional" asymptotic behavior of the vdW interaction energy which dominates the binding at very large distances (*e.g.*, beyond 10–20 nm in bilayer graphene) [16]. Moreover, Misquitta *et al.* [17, 18] demonstrated that upon closure of the band gap, semiconducting nanowires may also exhibit unconventional power laws as a function of the interwire distance D, namely $\sim D^{-2}$ at intermediate separations, followed by asymptotic convergence to the pairwise-additive D^{-5} limit for large interwire separations.

Here we significantly revise and extend these seminal

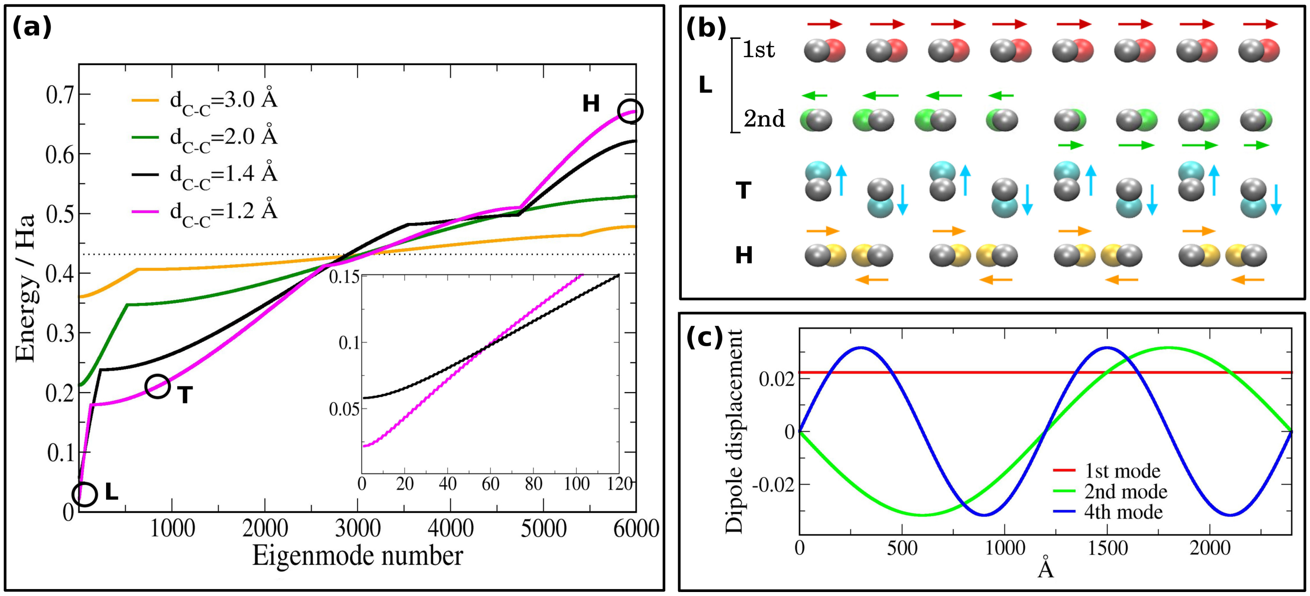

FIG. 1. **(a)** Energy eigenvalue spectrum corresponding to the $3N$ collective eigenmodes of the many-body dispersion (MBD) model [19, 20] (plotted in ascending order) for 1D carbyne-like atomic wires comprised of $N = 2000$ C atoms (subject to periodic boundary conditions) and several values of the interatomic C–C distance, $d_{\mathrm{C-C}}$, ranging from 1.2 Å (the C–C bond length in acetylene) to 3.0 Å. For reference, the independent atom value of $\omega_{\mathrm{C}} = 0.43$ Ha is provided by the dotted line. A more detailed view of the low-energy portion of the spectrum is provided in the inset (with the same units). **(b)** Schematic illustration of several representative *low-energy* (**L**), *transverse* (**T**), and *high-energy* (**H**) collective MBD eigenmodes, as indicated in **(a)**. The colored spheres represent charge displacements with respect to the equilibrium atomic positions (depicted in gray). **(c)** Longitudinal dipole displacements of several illustrative low-energy collective MBD eigenmodes (in arbitrary units) with respect to the wire coordinate for $d_{\mathrm{C-C}} = 1.2$ Å. Due to the inversion symmetry of this system, every eigenmode is doubly-degenerate except the lowest-energy longitudinal mode (depicted in red). Consistent with a normal mode analysis of a dipolar-coupled system with this underlying topology, the number of nodes present in a given MBD eigenmode is directly correlated with its relative location in the energy eigenvalue spectrum.

asymptotic results to the *finite distance* regime between nanostructures, motivated by the fact that interactions at such distances (as opposed to asymptotic separations) determine the structural, mechanical, spectroscopic, and (opto)electronic properties at the nanoscale. By considering a series of relevant zero-, one- and two-dimensional systems, including proteins, carbyne-like wires and nanotubes, graphenic layers, and MoS_2, we demonstrate that the vdW interactions between non-metallic nanostructures exhibit a wavelike nature that extends well beyond the low-order particle- or fragment-based IPT paradigm. In doing so, we provide further insight into the roles played by dimensionality, topology, and polarizability in determining the magnitude of these fundamental interactions at the nanoscale.

In systems where electrons are well-described by a localized representation of the occupied space (*e.g.*, systems with finite band gaps), collective charge density fluctuations stem from the dynamically correlated motions of local dipolar excitations. Accordingly, we project the valence electronic response in a given nucleoelectronic system onto a set of N interacting atomic response functions, as outlined by the many-body dispersion (MBD) scheme [19]. This approach has been applied with great success to the computation of polarizabilities [21] and dispersion interactions in weakly bound systems [22, 23], and has recently been extended to arbitrary non-metallic molecules, solids, and nanostructures by utilizing spatially-distributed polarizabilities [19, 20]. The advantage of the MBD method resides in an efficient and accurate quantum mechanical parameterization of the valence electronic response in terms of coupled atomic dipolar fluctuations [24, 25], allowing for a *chemically accurate* treatment of molecules and extended systems when utilized in conjunction with state-of-the-art exchange-correlation (XC) functionals in density-functional theory [2, 3, 6, 20, 26–29].

Within the MBD model, the long-range correlation energy, $E_{\mathrm{vdW}}^{\mathrm{LR}}$, is computed *via* the adiabatic connection fluctuation-dissipation theorem (ACFDT) [24, 30] as

$$E_{\mathrm{vdW}}^{\mathrm{LR}} = -\frac{1}{2\pi}\int_0^\infty d\omega \int_0^1 d\lambda \, \mathrm{Tr}[(\chi_\lambda - \chi_0)v] \, , \qquad (1)$$

in which χ_0 is the bare response function for a system of non-interacting atoms and χ_λ is the interacting response function "dressed" by the rescaled and rangeseparated [19] Coulomb interaction, λv (the convention $m_e = \hbar = q = 1/(4\pi\epsilon_0) = 1$ is adopted throughout the manuscript). Within the dipole approximation, Eq. (1) can be computed exactly and is equivalent to diagonalization of the following coupled dipolar Hamiltonian [24],

$$\hat{H} = -\frac{1}{2}\sum_{p=1}^{N}\nabla^2_{\boldsymbol{\mu}_p} + \frac{1}{2}\sum_{p=1}^{N}\omega_p^2\boldsymbol{\mu}_p^2 + \sum_{p>q}^{N}\omega_p\omega_q\sqrt{\alpha_p^0\alpha_q^0}\,\boldsymbol{\mu}_p\mathfrak{T}_{pq}\boldsymbol{\mu}_q \,, \tag{2}$$

in which each atom p is characterized by a static dipole polarizability, α_p^0, and a characteristic excitation frequency, ω_p, and $\boldsymbol{\mu}_p$ represents the mass-weighted displacement of atom p from its equilibrium position, $\mathbf{R}_p$. The first two terms in this Hamiltonian correspond to the single-particle kinetic and potential energies, respectively, while the last term describes the coupling between atoms p and q *via* the dipole-dipole interaction tensor, $\mathfrak{T}_{pq} = \nabla_{\mathbf{R}_p} \otimes \nabla_{\mathbf{R}_q} v(R_{pq})$, wherein $v(R_{pq})$ is the Coulomb interaction at the interatomic distance $R_{pq} = |\mathbf{R}_p - \mathbf{R}_q|$ [24]. The long-range correlation energy is then computed as the energetic difference between the eigenfrequencies of the collective modes of the fully interacting system, $\overline{\omega}_i$, and the characteristic excitation frequencies of the isolated atoms, ω_p.

We begin our investigation into the nature of vdW interactions at the nanoscale with a detailed analysis of the collective density fluctuations sustained in a linear (1D) carbyne-like atomic wire comprised of 2000 atoms subject to periodic boundary conditions. From Fig. 1(**a**), we first observe that such finite atomic wires are characterized by a set of very low-energy collective eigenmodes (albeit with non-zero energy eigenvalues). The minimum energy (gap) of such modes approaches the independent atom value ($\omega_{\mathrm{C}} = 0.43$ Ha) at large C–C distances, $d_{\mathrm{C-C}}$, but decreases to approximately $1/20^{\mathrm{th}}$ of this value at $d_{\mathrm{C-C}} = 1.2$ Å, the C–C bond length in acetylene. Due to charge conservation, the quantity $\overline{\alpha}_i^0\,\overline{\omega}_i^2$ (with $\overline{\alpha}_i^0$ and $\overline{\omega}_i^2$ denoting the static dipole polarizability and resonant frequency of the i^{th} eigenmode, respectively) must be equivalent for every MBD eigenmode, as initially set by the independent atomic value of $\alpha_{\mathrm{C}}^0\omega_{\mathrm{C}}^2$. The lowest energy eigenmode is therefore characterized by a very high static dipole polarizability (*i.e.*, up to ~ 400 times that of a single C atom), which is strongly indicative of a marked delocalization of the charge density fluctuations over the *entire* wire. In this case, the low dimensionality and particular topology of this nanostructure is crucial for sustaining coherent delocalized fluctuations along the length of the wire. As depicted in Fig. 1(**b**)–(**c**), these charge density fluctuations result from strongly enhanced (*head-to-tail*) dipole-dipole coupling along the longitudinal axis of the atomic wire, which leads to significant anisotropy in the associated polarizability tensor [31].

To further expand on these observations, we now analyze the low-energy spectrum of the collective MBD eigenmodes characteristic of this low-dimensional nanostructure. As illustrated in Fig. 1(**b**)–(**c**), these low-energy modes correspond to coherent dipolar fluctuations aligned along the entire wire, having negligible components orthogonal to the longitudinal axis. Consistent with a normal mode analysis of a dipolar-coupled system with this underlying topology, higher-energy modes correspond to polarization waves with an increasing number of nodes. At the highest energies (*i.e.*, beyond the shoulder in the spectrum of Fig. 1(**a**)), the collective MBD eigenmodes have sizable transverse components and contribute negligibly to the coherent dipolar fluctuations aligned along the wire.

Upon compression of the carbyne wire (*i.e.*, by varying $d_{\mathrm{C-C}}$ from 3.0 Å to 1.2 Å), the gap in the eigenvalue spectrum becomes visibly reduced and is accompanied by a corresponding increase in the slope of the dispersion curves. A gapless metallic dispersion [15] is thus approached, but never reached in the MBD model, a fact attributed to the intrinsic charge confinement of the valence atomic responses. We note here that a flat dispersion (approached only as $d_{\mathrm{C-C}} \to \infty$) would indicate a *localization* of the system response; with every eigenmode degenerate in energy, single-atom dipolar fluctuations would occur along the wire and result in a decorrelation of the atomic susceptibilities. Conversely, we observe from Fig. 1(**a**) that *intrawire* interactions can also induce non-trivial dispersion in the eigenvalue spectrum despite the absence of explicitly delocalized electrons, implying a marked non-locality in the collective dipolar response within the MBD model. This collective behavior stems from a subtle balance between the kinetic and potential energy operators in Eq. (2). Upon compression of the carbyne wire, the kinetic energy term increases in comparison to the potential energy, leading to large amplitude oscillator motions induced by many-body kinetic energy contributions. In addition, an analysis of the exact two-atom MBD solution reveals an underlying dependence of the long-range correlation energy on the quantity $\alpha_{\mathrm{C}}d_{\mathrm{C-C}}^{-3}$; as such, the effect of varying the interatomic distance is expected to be qualitatively equivalent to an inversely proportional modification of the polarizability.

The analysis presented above already provides strong evidence of the wavelike nature of vdW interactions in low-dimensional non-metallic nanostructures. To investigate this aspect further, we now consider the case of two mutually interacting parallel carbyne-like wires. In Fig. 2, the resulting *interwire* interaction energy power laws are plotted as a function of the interwire separation, D (and for several values of $d_{\mathrm{C-C}}$), and exhibit strong deviations from the D^{-5} behavior predicted by widely employed vdW approaches based on pairwise additivity. This macroscopic effect goes beyond a simple renormalization of Hamaker constants and results from a theoretical account of both *intra-* and *inter-*wire many-body vdW interactions on an equal footing. As clearly seen

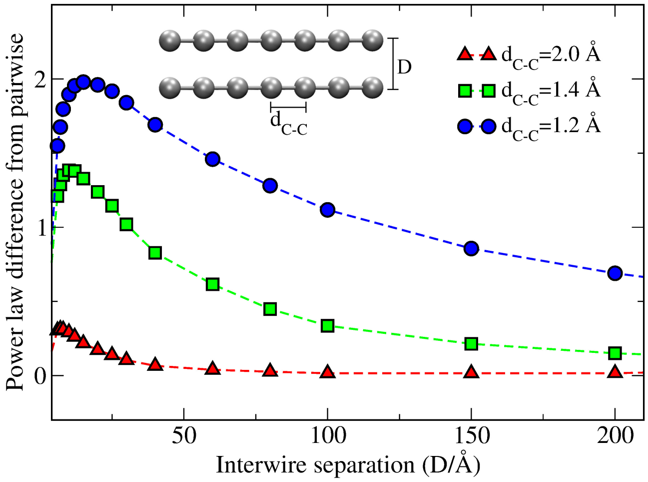

FIG. 2. Difference of the many-body dispersion (MBD) model [19, 20] interwire interaction energy power laws from the pairwise-additive asymptotic prediction for two parallel 1D carbyne-like atomic wires as a function of the interwire separation D and several values of the interatomic C–C distance, $d_{\mathrm{C-C}}$ (ranging from 1.2 Å to 2.0 Å). Over a range of relevant nanoscale distances, there are strong deviations from the well-known interwire interaction energy power law of D^{-5}, as predicted by widely employed pairwise-additive vdW models.

in Fig. 2, these interaction energy power law modifications become even more pronounced upon compression of the carbyne wire, reaching $\sim D^{-3}$ for interwire separations between 1–3 nm (with $d_{\mathrm{C-C}} = 1.2$ Å), while still not converging to the pairwise-additive asymptote at interwire separations exceeding 20 nm. Such interaction energy power law modifications are particularly relevant at the nanoscale and can be understood as resulting from long-range electrodynamic coupling between the collective longitudinal modes (dipole waves) delocalized along the entirety of each carbyne-like wire. These wavelike interactions are simply absent in localized particle- or fragment-based models for vdW interactions, despite the fact that their inclusion is crucial for an accurate theoretical description of these fundamental interactions in low-dimensional non-metallic nanostructures. We note here that these findings resemble the results obtained with approximate many-body models of metallic chains that *explicitly* account for the delocalized wavelike nature of metallic electrons [4, 15, 17, 32], which implies that a collective dipolar response with markedly non-local character can also be utilized to predict the emergence of wavelike dynamical electron correlation in non-metallic systems.

To further understand the wavelike nature of the vdW interaction between carbyne wires, let us now consider an analytic model for this interaction in more detail. At sufficiently large D, the *interwire* Coulomb interaction in the continuum approximation is given by $w_{12} = 2K_0(qD)$, in which K_0 is a modified Bessel function and q is the magnitude of the wave vector parallel to the longitudinal wire axes [15]. Within the random-phase approximation (RPA), one can account for the interwire coupling on the response function of a single wire, χ_1, *via* $\chi_1^2 w_{12}^2 = 1$, which predicts a splitting of $\overline{\omega}(q)$ into eigenfrequencies that correspond to coupled dipolar fluctuations that are either aligned ($\overline{\omega}_+$) or anti-aligned ($\overline{\omega}_-$) with respect to the two parallel wires (*i.e.*, $\overline{\omega}_\pm(q) = \overline{\omega}(q)\sqrt{1 \pm \overline{\alpha}^0(q)T(q)}$, wherein $T(q)$ is the interwire dipole-dipole interaction derived from w_{12}). Neglecting the higher-energy transverse eigenmodes which provide smaller contributions to the interwire interaction, the interaction energy between carbyne-like wires of length L can then be computed in the non-retarded regime as

$$E^{\mathrm{LR}}_{\mathrm{vdW},12} = \frac{L}{4\pi} \int dq \, \left(\overline{\omega}_+(q) + \overline{\omega}_-(q) - 2\overline{\omega}(q)\right) , \qquad (3)$$

which in turn can be expanded to second order in the interaction at large D, yielding:

$$E^{\mathrm{LR}(2)}_{\mathrm{vdW},12} = -\frac{\left(\alpha^0_{\mathrm{C}}\omega^2_{\mathrm{C}}\right)^2 L}{16\pi d^2_{\mathrm{C-C}}} \int dq \, \frac{K_0^2(qD)q^4}{\overline{\omega}^3(q)} \, . \qquad (4)$$

A q-space decomposition of the integrand in Eq.(4) is provided in Fig. 3 and clearly illustrates that the power law governing the interwire interaction energy has a non-trivial dependence on D that originates from a summation over individual reciprocal-space contributions, each of which corresponds to a normal mode of the system with a *different* characteristic decay rate. This observation is in stark contrast to the determination of the interwire interaction energy from approximate particle- or fragment-based pairwise approaches, in which each contribution has the same D^{-5} power law decay. As such, this analysis is also strongly indicative that the complex interwire interaction energy power laws displayed in Fig. 2 can *only* be correctly described by models which allow for delocalized wavelike fluctuations of the charge density. In this regard, even state-of-the-art non-local XC functionals [33, 34], which describe long-range electron correlation effects in a pairwise-additive fashion, would completely miss the interaction energy profile in Fig. 2.

To gain a more detailed understanding of the power laws displayed in Fig. 2, we note that the asymptotic behavior of the interwire interaction energy is largely influenced by $\overline{\omega}(q)$, the *single* wire dispersion appearing in the integrand of Eq. (4). In fact, a first estimate of the decay rate of $E^{\mathrm{LR}(2)}_{\mathrm{vdW},12}$ can be obtained by fitting the dispersion law with a single exponent, *i.e.*, as $\overline{\omega}(q) \propto q^{\delta}$, which directly leads to the finding that $E^{\mathrm{LR}(2)}_{\mathrm{vdW},12} \propto D^{5-3\delta}$ upon variable substitution of $q' = q/D$. Physically speaking, the quantity $K_0(qD)$ governs the interwire interaction

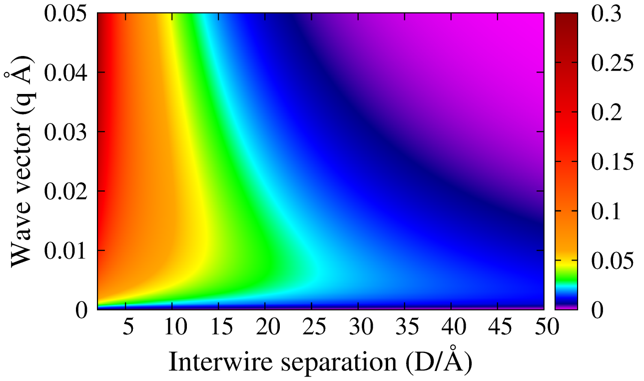

FIG. 3. Reciprocal-space decomposition analysis of the integrand required for computing the second-order interwire interaction energy in Eq.(4). Assuming linear dispersion, the decay rate of the integrand with respect to the interwire separation, D, exhibits a non-trivial dependence on the momentum, q, which is responsible for the observed power law decay of the interwire interaction energy, $E^{\mathrm{LR}(2)}_{\mathrm{vdW},12}$. At large D, only small q contributions significantly influence $E^{\mathrm{LR}(2)}_{\mathrm{vdW},12}$, so that D effectively determines the scale of *relevant* momenta. In this plot, the integrand has been rescaled by a constant factor of $\overline{\omega}(0)^3$ and is given in a.u.

by introducing a momentum cutoff at $q \sim 1/D$ and the resultant integration over the infinitesimal contributions $q^4/\overline{\omega}^3(q)$ up to the momentum cutoff controls the scaling of $E^{\mathrm{LR}(2)}_{\mathrm{vdW},12}$ with respect to D. In particular, while a linear plasmon dispersion leads (up to logarithmic corrections) to a D^{-2} decay [15] in metallic wires, the slightly sublinear dispersion observed here for $d_{\mathrm{C-C}} = 1.2$ Å (see the inset in Fig. 1(**a**) after the initial energetic gap) is consistent with a $\sim D^{-2.8}$ power law and is in qualitative agreement with the numerical evidence provided by the MBD model in Fig. 2. We note in passing that despite this initial deviation from D^{-5}, the power law at large distances again tends toward the pairwise-additive asymptote, although deviations still persist at interwire separations exceeding 20 nm. A direct account of this phenomenon follows from Fig. 3: due to the decay of $K_0(qD)$ with respect to the quantity qD, only very small values of q will contribute to the interwire interaction energy at large D (*cf.* Eq. (4)). In fact, only those wave vectors close to the gap (in which $\omega(q) \sim$ *const.*) will be of relevance in recovering the asymptotic D^{-5} limit. Hence, the pairwise-additive limit can only be approached in the presence of a *flat* dispersion, wherein the localization of the system response to single-atom dipolar fluctuations occurring along the individual wires would actually validate the fundamental particle-based assumption that the vdW interaction energy can be described as a summation over induced atomic dipole—induced atomic dipole contributions.

Interestingly, the results of the above analysis are quite general and are not simply intrinsic properties of the MBD coupled dipolar Hamiltonian (see Eq. (2)). In this regard, the same wavelike character of vdW interactions at the nanoscale are observed when the *qualitatively* different tight binding (TB) model [17] is utilized for the single nanowire response. Within this approach, the individual atomic wires are described by a two-site nearest-neighbor interaction that can be tuned (by manipulating the β_1 and β_2 free-parameter space) to reproduce both the metallic (symmetric interactions *via* $\beta_2/\beta_1 = 1$) and insulating (asymmetric/single-sided interactions *via* $\beta_2/\beta_1 = 0$) limits. A second-order perturbative treatment of the *interwire* interaction energy leads to power laws that describe these two respective limits, *i.e.*, $\sim D^{-2}$ for metallic nanowires and $\sim D^{-5}$ for insulating nanowires with *flat* energy bands, as depicted in Fig. 4. In analogy with the MBD model, the TB response becomes markedly non-local in the metallic limit, the regime in which the largest deviations from the pairwise-additive $\sim D^{-5}$ power law are expected. Conversely, a substantial localization of the response is recovered in the insulating limit, in which the pairwise approximation becomes asymptotically valid. Comparisons of the interwire interaction energy power laws provided in Figs. 2 and 4 clearly demonstrate semi-quantitative agreement between the qualitatively different MBD and TB models

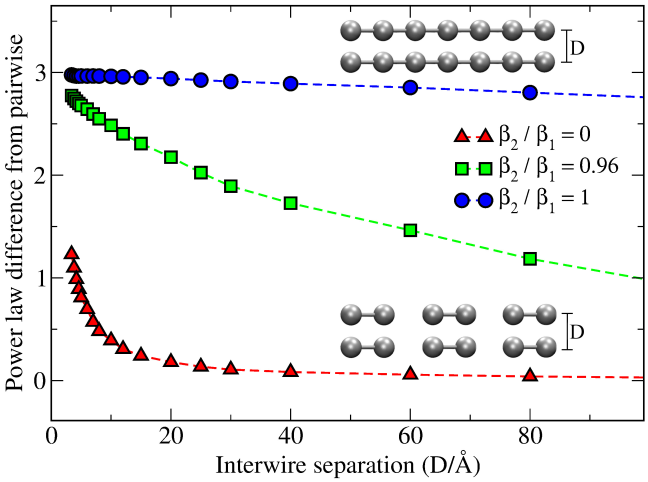

FIG. 4. Difference of the tight-binding (TB) model [17] interwire interaction energy power laws from the pairwise-additive asymptotic prediction for two parallel 1D carbyne-like atomic wires as a function of the interwire separation D. With the interatomic C–C distance set to $d_{\mathrm{C-C}} = 2.0$ Å, the two limiting cases of insulating (with $\beta_2/\beta_1 = 0$) and metallic ($\beta_2/\beta_1 = 1$) nanowires were considered, along with an intermediate case ($\beta_2/\beta_1 = 0.96$). As found above with the qualitatively different MBD model, there are strong deviations from the well-known interwire interaction energy power law of D^{-5}, as predicted by widely employed pairwise-additive vdW models, over a range of relevant nanoscale distances. For a more detailed discussion of the TB model utilized herein, see the accompanying SUPPLEMENTARY MATERIAL.

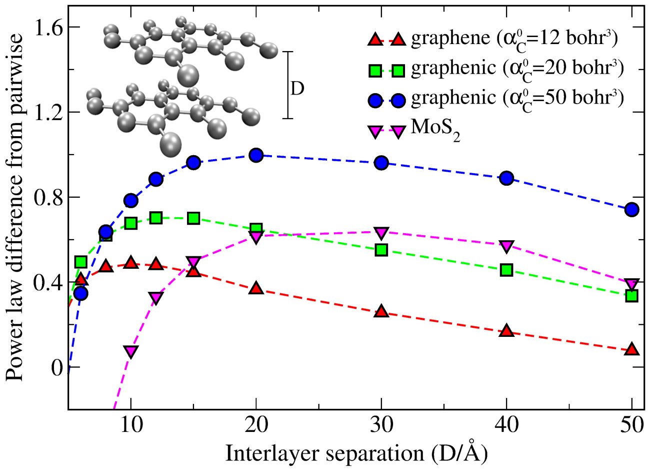

FIG. 5. Difference of the many-body dispersion (MBD) model [19, 20] interlayer interaction energy power laws from the pairwise-additive asymptotic prediction for two parallel 2D graphenic layers and MoS_2 as a function of the interlayer separation D. To investigate these power law deviations in highly polarizable 2D materials, several values of the static atomic dipole polarizability, α_C^0, were considered for the graphenic layers, ranging from 12 bohr^3 (the static atomic dipole polarizability in graphene) to 50 bohr^3. As found above for the case of interacting parallel 1D nanowires, there are significant deviations from the well-known interlayer interaction energy power law of D^{-4}, as predicted by widely employed pairwise-additive vdW models, over a range of relevant nanoscale distances.

and is strongly indicative of the universality of the wave-like nature of vdW interactions between nanostructures.

While the results above were obtained for model 1D carbyne-like wires, our calculations suggest that collective charge density fluctuations will also strongly influence the behavior of strained hydrocarbon polymers and inorganic wires comprised of polarizable elements such as phosphorus, silicon, or germanium. To further elucidate the roles of dimensionality and topology on determining interaction power laws across distances relevant at the nanoscale, we carried out a study of layered 2D materials, including graphenic sheets of varying polarizability, as well as bilayer MoS_2. Although a smaller power law reduction is expected in bilayer graphene due to its higher dimensionality, a $D^{-3.5}$ decay is found for interlayer distances of 0.8–1.5 nm, with convergence to the conventional D^{-4} power law only achieved for interlayer distances larger than 5 nm (see Fig. 5). Overall, the interlayer interaction power laws were found to be intermediate between D^{-3} and the pairwise-additive D^{-4} asymptote, which are induced by gapless π states and expected to be valid in the case of finite-gap doped graphene [35, 36]. Increasing the polarization response of the graphenic sheets to effectively model highly polarizable 2D materials leads to significant delocalization in the system response; for $\alpha_C^0 = 50$ bohr^3, the interaction power law exhibits an extended plateau of $\sim D^{-3}$ at interlayer separations in the range of 1.5–4.0 nm—distances which are again quite relevant to interactions at the nanoscale.

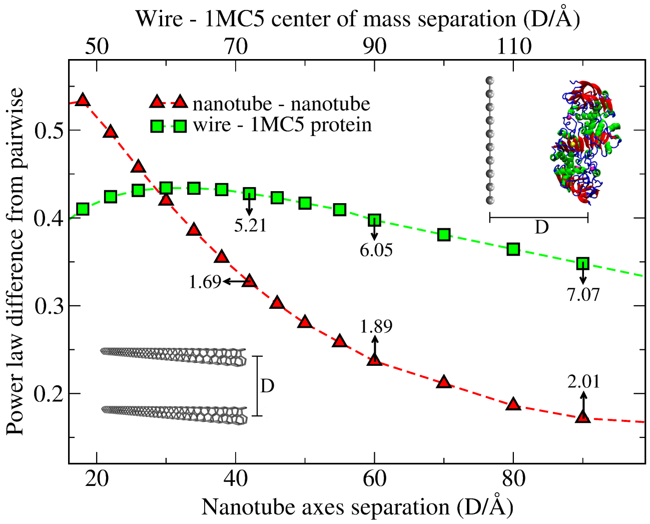

FIG. 6. Difference of the many-body dispersion (MBD) model [19, 20] interlayer interaction energy power laws from the pairwise-additive asymptotic prediction for two parallel (3,3) nanotubes and a protein (1MC5) interacting with a monoatomic wire as a function of the mutual center-of-mass separation D. The ratio between MBD and pairwise energies $E_{\rm MBD}/E^{(2)}$ is indicated for 1MC5-wire system for various separations. This ratio grows with increasing separation between objects.

As the last example, we extend our observations on the crucial importance of many-body interactions to biological systems and nanotubes. As Figure 6 demonstrates, for a protein 1MC5 (Human glutathione-dependent formaldehyde dehydrogenase) interacting with a nanowire, the decay of the MBD energy is pronouncedly slower when compared to the widely used pairwise approximation. In addition, the energy ratio $E_{\rm MBD}/E^{(2)}$ is large and grows as a function of the separation between the protein and the wire, demonstrating a non-trivial coupling between delocalized fluctuations on the protein and the wire.

The analysis presented herein demonstrates the remarkable ability one has in engineering the interaction energy power laws in low-dimensional nanosystems by modifying their underlying dimensionality, topology, and response properties. Moreover, the present findings suggest that complex power laws could also play an important role in numerous biologically relevant systems that are characterized by low dimensionality, including phospholipid aggregates and bilayers [37], or even the subnanometer spatula-shaped structures determining the peculiar pedal adhesion in the gecko [38]. In summary, this study provides strong evidence that the ubiquitous vdW forces between polarizable non-metallic nanostructures can be more completely understood in terms of collective interactions between wavelike charge density fluctuations, rather than simply a summation over pairwise interactions between instantaneous particle-like dipolar fluctuations. In analogy with metallic systems, the marked non-locality of the valence electronic response in low-dimensional polarizable nanostructures is reflected in the emergence of collective modes that span the entire system. It is these delocalized wavelike charge density fluctuations that are responsible for the non-trivial interaction energy power laws observed herein, which significantly deviate from the predictions of standard pairwise-additive vdW approximations. As such, wavelike fluctuations govern the magnitude of these ubiquitous interactions at large, but finite, distances of relevance at the nanoscale. These findings reveal a smooth transition from a system comprised of independent atoms to the collective fully interacting limit, thereby providing a potential pathway for the tuning of the fundamental non-covalent vdW interactions responsible for the assembly of complex polarizable nanostructures.

All authors are grateful for financial support from the European Research Council (ERC) Starting Grant VDW-CMAT. R.D. is also grateful for additional financial support through a startup grant from Cornell University. A.A. would also like to acknowledge Flavio Toigo and Pier Luigi Silvestrelli for useful discussions.

---

[1] V. A. Parsegian, *Van der Waals forces: A Handbook for Biologists, Chemists, Engineers and Physicists* (Cambridge University Press, 2005).
[2] A. Tkatchenko, Adv. Func. Mater. **25**, 2054 (2015).
[3] A. M. Reilly and A. Tkatchenko, Chem. Sci. **6**, 3289 (2015).
[4] Y. V. Shtogun and L. M. Woods, J. Phys. Chem. Lett. **1**, 1356 (2010).
[5] W. Gao and A. Tkatchenko, Phys. Rev. Lett. **114**, 096101 (2015).
[6] A. M. Reilly and A. Tkatchenko, Phys. Rev. Lett. **113**, 055701 (2014).
[7] N. Ferri, R. A. DiStasio Jr., A. Ambrosetti, R. Car, and A. Tkatchenko, Phys. Rev. Lett. **114**, 176802 (2015).
[8] A. J. Stone, *The Theory of Intermolecular Forces* (Oxford University Press, 2nd Edition, 2013).
[9] C. A. Silvera-Batista, R. G. Larson, and N. A. Kotov, Science **350**, 6257 (2015).
[10] P. Loskill, H. Hähl, T. Faidt, S. Grandthyll, F. Müller, and K. Jacobs, Adv. Coll. Interf. Sci. **179**, 107 (2012).
[11] P. Loskill, J. Puthoff, M. Wilkinson, K. Mecke, K. Jacobs, and K. Autumn, J. R. Soc. Interface **10**, 20120587 (2013).
[12] S. Tsoi, P. Dev, A. L. Friedman, R. Stine, J. T. Robinson, T. L. Reinecke, and P. E. Sheehan, ACS Nano **8**, 12410 (2014).
[13] G. Rance, D. Marsh, S. Bourne, T. Reade, and A. Khlobystov, ACS Nano **4**, 4920 (2010).
[14] C. Wagner, N. Fournier, V. G. Ruiz, C. Li, K. Müllen, M. Rohlfing, A. Tkatchenko, R. Temirov, and F. S. Tautz, Nature Comm. **5**, 5568 (2014).
[15] J. F. Dobson, A. White, and A. Rubio, Phys. Rev. Lett. **96**, 073201 (2006).
[16] J. F. Dobson, T. Gould, and G. Vignale, Phys. Rev. X **4**, 021040 (2014).
[17] A. J. Misquitta, J. Spencer, A. J. Stone, and A. Alavi, Phys. Rev. B **82**, 075312 (2010).
[18] A. J. Misquitta, R. Maezono, N. D. Drummond, A. J. Stone, and R. Needs, Phys. Rev. B **89**, 045140 (2014).
[19] A. Tkatchenko, R. A. DiStasio Jr., R. Car, and M. Scheffler, Phys. Rev. Lett. **108**, 236402 (2012).
[20] A. Ambrosetti, A. M. Reilly, R. A. DiStasio Jr., and A. Tkatchenko, J. Chem. Phys. **140**, 18A508 (2014).
[21] J. Applequist, K. Sundberg, M. Olson, and L. Weiss, J. Chem. Phys. **70**, 1240 (1979).
[22] W. L. Bade, J. Chem. Phys. **27**, 1280 (1957).
[23] A. G. Donchev, J. Chem. Phys. **125**, 074713 (2006).
[24] A. Tkatchenko, A. Ambrosetti, and R. A. DiStasio Jr., J. Chem. Phys. **138**, 074106 (2013).
[25] A. Jones, J. Crain, V. Sokhan, T. Whitfield, and G. Martyna, Phys. Rev. B **87**, 144103 (2013).
[26] A. M. Reilly and A. Tkatchenko, J. Phys. Chem. Lett. **4**, 1028 (2013).
[27] A. Ambrosetti, D. Alfè, R. A. DiStasio Jr., and A. Tkatchenko, J. Phys. Chem. Lett. **5**, 849 (2014).
[28] R. A. DiStasio Jr., O. A. von Lilienfeld, and A. Tkatchenko, Proc. Natl. Acad. Sci. USA **109**, 14791 (2012).
[29] R. A. DiStasio Jr., V. V. Gobre, and A. Tkatchenko, J. Phys.: Condens. Matter **26**, 213202 (2014).
[30] J. F. Dobson, J. Wang, B. P. Dinte, K. McLennan, and H. M. Le, Int. J. Quantum Chem. **101**, 579 (2005).
[31] V. V. Gobre and A. Tkatchenko, Nat. Commun. **4**, 2341 (2013).
[32] R.-F. Liu, J. G. Angyan, and J. F. Dobson, J. Chem. Phys. **134**, 114106 (2011).
[33] M. Dion, H. Rydberd, E. Schröder, D. C. Langreth, and B. I. Lundqvist, Phys. Rev. Lett. **92**, 246401 (2004).
[34] K. Berland, V. R. Cooper, K. Lee, E. Schröder, T. Thonhauser, P. Hyldgaard, and B. I. Lundqvist, Rep. Prog. Phys. **78**, 066501 (2015).
[35] J. Dai, J. Yuan, and P. Giannozzi, Appl. Phys. Lett. **95**, 232105 (2009).
[36] P. A. Denis, Chem. Phys. Lett. **508**, 95 (2011).
[37] L. Lis, M. McAlister, N. Fuller, R. Rand, and V. Parsegian, Biophys. J. **37**, 657 (1982).
[38] K. Autumn, Y. Liang, S. Hsieh, W. Zesch, W. Chan, T. Kenny, R. Fearing, and R. Full, Nature **405**, 681 (2000).